

Bayesian inference with *tmbstan* for a state-space model with VAR(1) state equation

Yihan Cao* Jarle Tufto*

1 Introduction

Both frequentist and Bayesian statistical inference have been used for investigating ecological processes. In the frequentist framework, Template model builder (TMB, Kristensen et al., 2016), an R package developed for fast fitting complex linear or nonlinear mixed models, has gained the popularity recently, especially in the field of ecology which usually involves in modeling complicated ecological processes (for example Cadigan, 2015; Albertsen et al., 2016; Auger-Méthé et al., 2017). The combination of reverse-mode automatic differentiation and Laplace approximation for high-dimension integrals makes parameter estimation with TMB very efficient even for non-Gaussian and complex hierarchical models. TMB provides a flexible framework in model formulation and can be implemented even for statistical models where the predictor is nonlinear in parameters and random effect. However, the lack of capability of working in the Bayesian framework has hindered the adoption of it for Bayesians.

Within the Bayesian framework, the software package *Stan* (Gelman et al., 2015), a probabilistic programming language for statistical inference written in C++ attracts peoples attention. It uses the No-U-Turn Sampler (NUTS) (Hoffman & Gelman, 2014), an adaptive extension to Hamiltonian Monte Carlo (Neal et al., 2011), which itself is a generalization of the familiar Metropolis algorithm, to conduct sampling more efficiently through the posterior distribution by performing multiple steps per iteration. *Stan* is a valuable tool for many ecologists utilizing Bayesian inference, particularly for problems where BUGS (Lunn et al., 2000) is prohibitively slow (Monnahan et al., 2017). As such, it can extend the boundaries of feasible models for applied problems, leading to a better understanding of ecological processes. Fields that would likely benefit include estimation of individual and population growth rates, meta-analyses and cross-system comparisons, among many others.

Combining the merits of TMB and *Stan*, the new software package *tmbstan* (Monnahan & Kristensen, 2018) which provides MCMC sampling for TMB models was developed. This package provides ADMB and TMB users a possibility for making Bayesian statistical analysis when prior information on the unknown parameters is available. From the user's perspective, it implements NUTS sampling from a target density proportional to the product of marginal likelihood (computed by TMB or *Stan*) and the prior density specified by the user. The user has the flexibility to decide which random effects are integrated out via the Laplace approximation in TMB and then the TMB model is passed

*Centre for Biodiversity Dynamics, Department of Mathematical Sciences, Norwegian University of Science and Technology, 7491 Trondheim, Norway

to function Stan in the RStan package so that the rest of the parameters are integrated by Stan. This methodology might therefore potentially be more computationally efficient than using MCMC alone to integrate out all parameters. Monnahan and Kristensen (2018) introduced the *tmbstan* package, applied it to simulation studies and compared its capabilities (computational efficiency and the accuracy of Laplace approximation) with other platforms such as ADMB and TMB.

However, it is unclear that if Bayesian inference with arbitrary prior distribution implemented with Stan would perform comparatively with frequentist inference when modeling complex ecological processes. It is also unclear that when using *tmbstan*, if using the Laplace approximation to integrate latent variables is more computationally efficient than handling all latent variables via MCMC. In the case studies in Monnahan and Kristensen (2018), Laplace approximation turned out to reduce the computational efficiency of MCMC. Another issue arose in the case studies is that the Laplace approximation to the integration of random effects is not accurate to a degree and this could lead to biased parameter estimates or uncertainties in parameter estimation. To gain more insights on these issues, in this paper we conduct simulation studies and a case study in the context of modeling fluctuating and auto-correlated selection with state-space models (SSM). These forms of models are more generally increasingly used in ecology to model time-series such as animal movement paths and population dynamics (for example Cadigan, 2015; Albertsen et al., 2016; Auger-Méthé et al., 2017). Furthermore, following Cao, Visser, and Tufto (2019), we also use order-1 vector autoregressive model (VAR(1)) to model the unobserved states, which in our study are temporally fluctuating and potentially auto-correlated height, width and location of a Gaussian fitness function. This also allows us to make a further investigation into the issue of underestimation of the auto-correlation parameter in auto-regressive models shown in Chevin et al. (2015) and Cao et al. (2019).

Through the simulation and empirical studies, our paper aims to (1) compare estimates between frequentist inference and Bayesian inference under different simulation schemes; (2) investigate how the choice of prior influence Bayesian inference; (3) compare the computational efficiency of MCMC with and without integrating out some of the random effects via Laplace approximation.

2 Methodology

2.1 Model formulation

We consider a typical ecological process, the fluctuating selection in a bird species, the great tit (*Parus major*). We conduct the study in the context of temporally changing selection on the laying date with the number of fledglings as the fitness component, but it can be generalized to any episode of viability or fertility selection, or to overall selection through lifetime fitness. The discrete nonnegative variable, number of fledglings, is best modelled by distributions such as Poisson, or zero-inflated Poisson (for example Chevin et al., 2015; Cao et al., 2019). Within the framework of generalized linear models, the expected value of response variable is commonly linked to the linear predictors of biologically interest by logarithm. When both linear and quadratic effects of the traits are included, this leads to a Gaussian model of stabilizing selection. In this study, the number of fledglings in a specific brood is assumed to be Poisson distributed, $X_i|w_i \sim \text{Poisson}(w_i)$, where i indicates the breeding event. The fitness (the expected number of fledglings w_i)

of individuals with phenotype z_i is then given by

$$\ln w_i = \eta_t^{(\alpha)} - \frac{(z_i - \eta_t^{(\theta)})^2}{2(e^{\eta_t^{(\omega)}})^2}, \quad (1)$$

where $\eta_t^{(\alpha)}$, $\eta_t^{(\theta)}$ and $e^{\eta_t^{(\omega)}}$ (e based to guarantee positive) are parameters determining the logarithm of maximum fitness, optimum laying date and width of the fitness function in year t respectively. We further model $\eta_t^{(\alpha)}$, $\eta_t^{(\theta)}$ and $\eta_t^{(\omega)}$, the three stochastic processes as following:

$$\begin{aligned} \eta_t^{(\alpha)} &= \mu_\alpha + \sigma_\alpha \alpha_t, \\ \eta_t^{(\theta)} &= \mu_\theta + \sigma_\theta \theta_t, \\ \eta_t^{(\omega)} &= \mu_\omega + \sigma_\omega \omega_t. \end{aligned} \quad (2)$$

The elements of vector $\mu = (\mu_\alpha, \mu_\theta, \mu_\omega)^T$ are the means of the three processes. The stochastic processes $\alpha_t, \theta_t, \omega_t$ are assumed to be multivariate normal distributed $(\alpha_t, \theta_t, \omega_t)^T \sim$

$\mathbf{N}_3(\mathbf{0}, \mathbf{\Gamma}_0)$ with $\mathbf{\Gamma}_0 = \begin{bmatrix} 1 & \rho_{\alpha,\theta} & \rho_{\alpha,\omega} \\ \rho_{\alpha,\theta} & 1 & \rho_{\theta,\omega} \\ \rho_{\alpha,\omega} & \rho_{\theta,\omega} & 1 \end{bmatrix}$, where $\rho_{\alpha,\theta}$, $\rho_{\alpha,\omega}$ and $\rho_{\theta,\omega}$ indicate the correlations and are assumed to be mutually independent. $(\alpha_t, \theta_t, \omega_t)^T$ are further assumed to follow a first-order vector autoregressive (VAR(1)) process as below:

$$\begin{bmatrix} \alpha_t \\ \theta_t \\ \omega_t \end{bmatrix} = \mathbf{\Phi} \begin{bmatrix} \alpha_{t-1} \\ \theta_{t-1} \\ \omega_{t-1} \end{bmatrix} + \mathbf{w}_t, \quad (3)$$

where $\mathbf{\Phi}$ is 3×3 transition matrix and \mathbf{w}_t is a 3-dimensional vector of white noise. The covariance matrix of \mathbf{w}_t is calculated as $\mathbf{\Gamma}_0 - \mathbf{\Phi}\mathbf{\Gamma}_0\mathbf{\Phi}$. Correlations between the elements of \mathbf{w}_t are determined by both $\rho = (\rho_{\alpha,\theta}, \rho_{\alpha,\omega}, \rho_{\theta,\omega})$ and $\mathbf{\Phi}$. If ρ is $\mathbf{0}$ vector and $\mathbf{\Phi}$ is diagonal, then \mathbf{w}_t reduces to be three independent and identically distributed white noise processes. In this case, α_t, θ_t and ω_t simplify to three independent first-order autoregressive (AR(1)) processes. If ρ is $\mathbf{0}$ and all entries of $\mathbf{\Phi}$ are zero, both $(\alpha_t, \theta_t, \omega_t)^T$ and \mathbf{w}_t reduce to three independent and identically distributed white noise processes. In any case, our non-centered parameterization implies that the standard deviation of α_t, θ_t and ω_t is only determined by $\sigma_\alpha, \sigma_\theta$ and σ_ω respectively. We expect the non-centered parameterization yields simpler posterior geometries (Betancourt & Girolami, 2015) and will be much more efficient in terms of effective sample size when there is not much data (Stan Development Team, 2018b, chapter 20).

It is worth mentioning that one objective of this study is to provide another case study beyond the ones in Monnahan and Kristensen (2018). Therefore, even though α_t, θ_t and ω_t are assumed to be VAR(1) in the model, in the simulation study we consider only AR(1) θ_t and white noise of α_t and ω_t . The alternative simulation studies in which α_t, θ_t and ω_t are formulated as other possible stochastic processes can be conducted similarly and exhaustively, but that is an enormous amount of work in one single study. When α_t, θ_t and ω_t are assumed to be VAR(1), one caution to be taken is that all the eigenvalues of $\mathbf{\Phi}$ must lie in the unit circle to guarantee the VAR (1) process to be stationary (Wei, 2006). At last, in the simulation study, we assume that the model structure is known, which means that we already know θ_t is AR(1) process since the aim of the study is not to explore the structure of the true model.

2.2 Prior distribution

The priors are assumed to be independent to each other $\pi(\mu, \Phi, \Sigma) = \pi(\mu)\pi(\Phi)\pi(\Sigma)$. We take a normal $N(\mathbf{m}, q\mathbf{I}_3)$ prior distribution for the process mean vector $\mu = (\mu_\alpha, \mu_\theta, \mu_\omega)$ and input weak prior information on the process mean by taking $\mathbf{m} = \mathbf{0}$ and $q = 100$. Since in this study we assume constant $\eta_t^{(\alpha)}$ and $\eta_t^{(\omega)}$, $\phi_{\theta, \theta}$ is the only non-zero entry in Φ . We used truncated normal prior on $\phi_{\theta, \theta}$ since it outperforms Jeffreys' prior (Jeffreys & Jeffreys, 1961), g prior (Zellner, 1986) and natural conjugate prior (Schlaifer & Raiffa, 1961) in terms of posterior sensitivity using Highest Posterior Density Region (HPDR) criterion concluded from the simulation study in Karakani et al. (2016). Lei et al. (2011) also uses truncated normal distribution as subjective prior for the auto-regressive parameter in its AR (1) model. The mean and standard deviation of the truncated normal distribution are arbitrarily set to be 0 and 0.5 respectively.

For the variance of the error term σ_θ^2 (σ_α^2 and σ_ω^2 are assumed to be zero), two priors are used:

(1) half-Cauchy (0, 10) prior on σ_θ (Prior1);

(2) lognormal (1, 0.5) prior on σ_θ (Prior2).

These two priors are referred to Prior1 and Prior2 respectively in the rest of this paper. It is worth mentioning that we also tested uniform prior on $\log(\sigma_\theta)$ (non-informative improper prior which equals to $1/\sigma$ prior on σ (Gelman et al., 2006)) and inverse-gamma (1, 1) prior on σ_θ^2 (non-informative proper prior, also illustrated in (Gelman et al., 2006)), but both of them render an issue that the sampler traps in a subspace of the whole parameter space of $\log(\sigma_\theta)$ and results in numerous divergent transitions. It was potentially caused by the posterior becoming improper and consisting of a mode and an infinite low-posterior-density ridge extending to infinity as illustrated in Tufto et al. (2012). We thus in this study only consider the two proper informative priors (Prior1 and Prior2), while more information on the MCMC with inverse-gamma (1, 1) prior on σ_θ^2 is given in Supporting Information.

Note also that the scale parameters $\log(\sigma_\theta)$ is declared in the TMB template in the logarithmic format, but the half-Cauchy prior and lognormal prior contributed to the total likelihood with the log density in terms of σ_θ and for inverse-gamma prior, it is in terms of σ_θ^2 , where σ_θ is a positive transform $\sigma = e^{\log\sigma}$. Therefore, Jacobian adjustment (see chapter 20.3 in Stan Development Team (2018b) for Jacobian adjustment) was conducted by adding $\log\sigma_\theta$ to the total likelihood when half-Cauchy prior and lognormal prior are used. When testing inverse-gamma prior, it was $\log 2 + 2 \log \sigma_\theta$ added to the total likelihood.

2.3 Software implementation

The model is formulated with C++ and passed to TMB for frequentist inference. The model objective (fn) and gradient (gr) functions are fed to optimization function *nlmminb* with default setting to optimize the objective function.

For Bayesian inference, the TMB model objective and gradient functions are passed to *tmbstan* which uses the *stan* function and executes the No-U-Turn sampler (NUTS) algorithm by default to sample. Currently the other options are "HMC" (Hamiltonian Monte Carlo), and "Fixed_param". We ran the simulation study on a multicore computing server with enough RAM to avoid swapping to disk. The number of warmup iterations to be excluded when computing the summaries is set to 1000 and for total sample length, it is 3000. We thin each chain to every second sample and set the value

adapt_delta to 0.95, which is the average proposal acceptance probability Stan aims for during the adaption (warmup) period. We set a seed for each simulation including data set and tmbstan to make sure all the simulation results are reproducible.

Divergent transitions during sampling may occur due to a large step size in the sampler or a poorly parameterized model, meaning that the iteration of the MCMC sampler runs into numerical instabilities (Carpenter et al., 2017) and thus inferences will be biased. RStan team suggested that the problem may be alleviated by increasing the adapt_delta parameter (gives a smaller step size), especially when the number of divergent transitions is small (Stan Development Team, 2018a). In our simulation studies, we find it difficult to completely avoid divergent transitions across all data sets even though adapt_delta is increased to 0.95. Similar to Fuglstad, Hem, Knight, Rue, and Riebler (2019), we thus removed simulations where 0.1% or more divergent transitions in the iterations after warmup occur during the inference to avoid reporting biased results.

It is worth mentioning that the execution of Markov chains can be done in parallel. While the default of RStan is to use 1 core, the RStan team recommended to set it to as many processors as the hardware and RAM allow and at most one core per chain (Stan Development Team, 2018a). The simulations we run are done with a server that has 28 available cores. We thus set the number of cores to be 4 for the 4 Markov chains. However, since R is single threaded and for frequentist inference, optimization algorithm used in R function "nlminb" only uses one core of CPU, we thus only compare the computational efficiency between tmbstan with and without Laplace approximation and ignore the computational efficiency with "nlminb" to ensure fair comparisons.

3 Simulation scheme and results

3.1 Simulation scheme

All the data simulated are in natural units and considered to be biologically realistic according to the empirical studies of natural birds populations (e.g. Grant & Grant, 2002; Vedder et al., 2013). Samples were modeled from a population undergoing stabilizing selection with AR(1) θ_t , fixed $\eta_t^{(\alpha)}$ and $\eta_t^{(\omega)}$. Vector $\mu = (\mu_\alpha, \mu_\theta, \mu_\omega)^T$ is set to (2, 20, 3.5). The autocorrelation $\phi_{\theta,\theta}$ is set to 0.1, 0.4 and 0.7 (only positive values considered since the estimate of auto-correlation in temporal optimal laying date is positive, for example 0.3029 in Chevin et al. (2015) and 0.524 in Cao et al. (2019)), the variance of fluctuating optimal laying date σ_θ is set to 20.

For each value of $\phi_{\theta,\theta}$, $tmax = 25$ or 50 time points were simulated and for each time point the sample size was drawn from a Poisson distribution with mean $n = 25, 50$ or 100 individuals. We considered four combinations of $tmax$ and n , which are ($tmax = 25, n = 50$), ($tmax = 25, n = 100$), ($tmax = 50, n = 25$) and ($tmax = 50, n = 100$). These four combinations are referred as simulation setting 1, 2, 3, 4 respectively in the following sections. Similar to Cao et al. (2019), we neglected response to selection and used the same normal distribution for simulating individual phenotype each year. The phenotypic standard deviation before selection σ_z was set to 20, such that the strength of stabilizing selection $S = \sigma_z^2 / (e^{\eta^{(\omega)}})^2 + \sigma_z^2$ (e.g. Chevin et al., 2015) was 0.267. For each individual, its fitness was computed from its phenotype using equation (1), and its actual number of offspring was then drawn from a Poisson distribution with mean $w_t(z)$.

3.2 Frequentist vs. Bayesian estimates

The results of one single simulation obtained from maximum likelihood in the frequentist framework are compared with those from *tmbstan*. The summaries of the estimates with *tmbstan* are computed after dropping the warmup iterations and merging the draws from all the four chains. The frequentist and Bayesian estimates with different sample sizes and $\phi_{\theta,\theta} = 0.4$ are shown in Table 1, the estimates with other values of auto-correlation in θ_t ($\phi_{\theta,\theta} = 0.1$ and 0.7) can be found in Supporting Information.

From Table 1 we find that both frequentist and Bayesian inferences show good estimates for μ_α and μ_ω . It is interesting to see that the auto-correlation for θ_t is not always under-estimated under all settings (for example ($tmax = 25, n = 50$)), this can be also seen from the tables for parameter estimates in Supporting Information. Bayesian inference with Prior1 (half-Cauchy prior) generally reports smaller estimates of μ_θ than MLE and Prior2 (lognormal prior) but larger estimates of $\phi_{\theta,\theta}$ and $\log\sigma_\theta$. The estimates with MLE and Prior2 are close to each other while the estimates with Prior2 show fewer uncertainties for $\phi_{\theta,\theta}$ and $\log\sigma_\theta$ implied by the smaller standard errors in the brackets. Prior2 also reports smaller estimates for $\log\sigma_\theta$ compared with MLE and Prior1 since it puts very large weight on small values of the variance, as will be graphically demonstrated in section 3.4. We also find that $\phi_{\theta,\theta}$ and $\log\sigma_\theta$ are difficult parameters to estimate since none of these three techniques can estimate them accurately across all the cases. However, the estimates are based on one realization of simulation, the discrepancy between estimates to the true value would vary from simulation to simulation.

We also compare the estimates across the different sample sizes. We typically compare the estimates between setting ($tmax = 25, n = 50$) and ($tmax = 25, n = 100$), ($tmax = 50, n = 25$) and ($tmax = 50, n = 100$), ($tmax = 25, n = 100$) and ($tmax = 50, n = 100$). We find that increasing the mean sample size at each time point does not necessarily increase the certainty of the estimates, but the data set with increased time points ($tmax = 50, n = 100$) contains more information on the parameters of interest and thus reports more certain estimates compared with the data set with ($tmax = 25, n = 100$). The same conclusion can be also drawn by making similar comparisons among the estimates in Table S1 and S2 in Supporting Information.

We can also find from Table 1, Table S1 and S2 from Supporting Information that the Bayesian inference with Prior1 in some cases report 1 or 2 divergent transitions while with Prior2 there are no divergent transitions reported. This implies that the geometric shape of posterior likelihood with Prior1 is more challenging for sampling probably due to light tails and thus potentially leads to an incomplete exploration of the target distribution.

3.3 Bias Plot

The comparison between the estimates in the last section is based on one realization of the simulation. To make comparisons of estimates over more realizations, the simulation was repeated 50 times under the setting of ($tmax = 50, n = 25$). Due to divergent transitions, only 44 out of 50 replicates were kept and the replications with more than 0.1% divergent transitions (in 2000 iterations) were excluded from the analysis. For the estimate of $\phi_{\theta,\theta}$ and $\log\sigma_\theta$ in each replication, the bias was calculated in a frequentist framework as the absolute difference between the true value and the mean estimate from each inference technique. The absolute bias for $\phi_{\theta,\theta}$ and $\log\sigma_\theta$ are graphically displayed in the upper and lower plot in Fig. 1 respectively. From the upper plot we find that in most replications, Bayesian inference with Prior1 slightly outperforms the frequentist

Table 1: Frequentist and Bayesian estimates (standard errors) from the model with AR(1) θ_t , autocorrelation in θ_t $\phi_{\theta,\theta} = 0.4$, and different sample sizes ($(tmax = 25, n = 50)$, $(tmax = 25, n = 100)$, $(tmax = 50, n = 25)$ and $(tmax = 50, n = 100)$) from one realization of the simulation. For each sample size setting, the number of divergent transitions in the MCMC is also reported and is used as a measure of stability of the inference scheme. MLE stands for maximum likelihood estimate, Prior1 and Prior2 represent half-Cauchy (0, 10) and lognormal (1, 0.5) prior respectively.

$\phi_{\theta,\theta} = 0.4, tmax = 25, n = 50$				
Parameters	True value	MLE	Prior1	Prior2
no. divergent transitions	NA	NA	1	0
μ_α	2	2.017(0.015)	2.017(0.015)	2.016(0.015)
μ_θ	20	18.5(3.7)	18.3(5.1)	18.5(3.7)
μ_ω	3.5	3.472(0.028)	3.475(0.028)	3.469(0.028)
$\phi_{\theta,\theta}$	0.4	0.14(0.20)	0.23(0.23)	0.16(0.18)
$log\sigma_\theta$	2.996	2.77(0.15)	2.88(0.19)	2.70(0.14)
$\phi_{\theta,\theta} = 0.4, tmax = 25, n = 100$				
Parameters	True value	MLE	Prior1	Prior2
no. divergent transitions	NA	NA	2	0
μ_α	2	1.995(0.011)	1.995(0.012)	1.995(0.012)
μ_θ	20	20.2(8.7)	18.3(17.5)	20.1(7.4)
μ_ω	3.5	3.506(0.022)	3.508(0.022)	3.504(0.021)
$\phi_{\theta,\theta}$	0.4	0.50(0.17)	0.59(0.18)	0.46(0.13)
$log\sigma_\theta$	2.996	3.25(0.18)	3.43(0.28)	3.13(0.14)
$\phi_{\theta,\theta} = 0.4, tmax = 50, n = 25$				
Parameters	True value	MLE	Prior1	Prior2
no. divergent transitions	NA	NA	0	0
μ_α	2	1.974(0.015)	1.974(0.015)	1.973(0.015)
μ_θ	20	20.0(3.8)	19.8(4.9)	20.1(4.2)
μ_ω	3.5	3.520(0.032)	3.523(0.032)	3.515(0.031)
$\phi_{\theta,\theta}$	0.4	0.42(0.14)	0.48(0.15)	0.42(0.13)
$log\sigma_\theta$	2.996	2.84(0.13)	2.92(0.16)	2.79(0.13)
$\phi_{\theta,\theta} = 0.4, tmax = 50, n = 100$				
Parameters	True value	MLE	Prior1	Prior2
no. divergent transitions	NA	NA	0	0
μ_α	2	1.9865(0.0076)	1.9864(0.0076)	1.9861(0.0076)
μ_θ	20	20.7(3.9)	20.0(5.0)	20.7(4.1)
μ_ω	3.5	3.512(0.015)	3.513(0.015)	3.510(0.015)
$\phi_{\theta,\theta}$	0.4	0.41(0.13)	0.47(0.15)	0.41(0.12)
$log\sigma_\theta$	2.996	2.89(0.12)	2.97(0.17)	2.85(0.11)

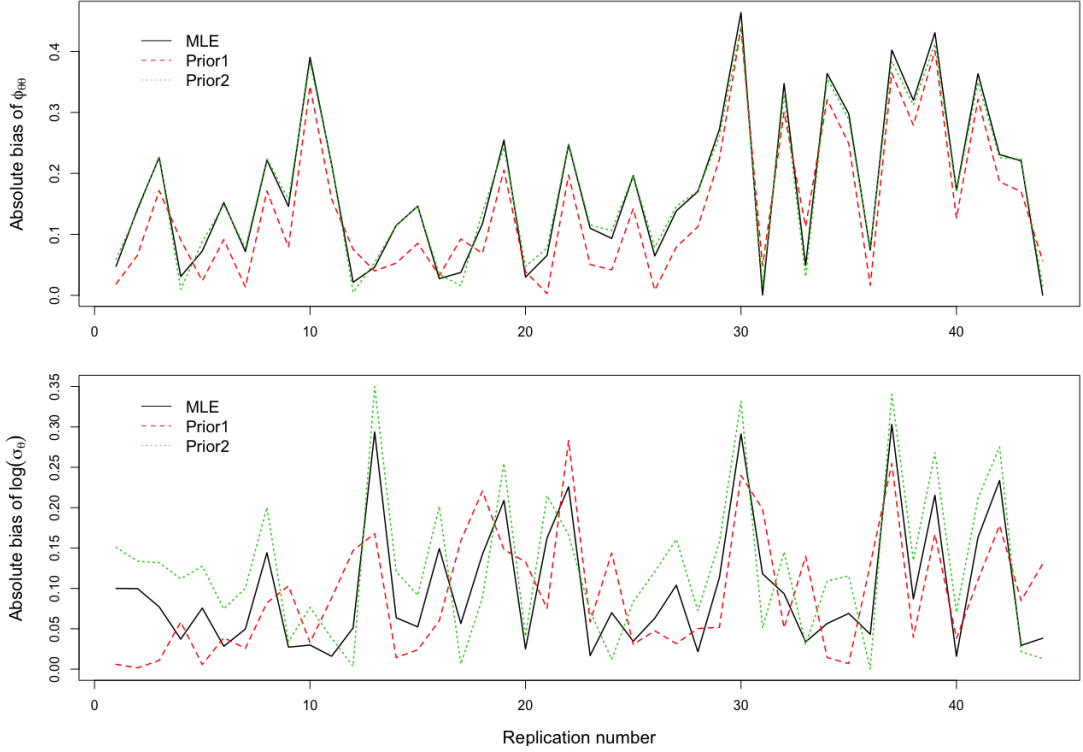


Figure 1: Bias plots for the auto-regressive parameter $\phi_{\theta,\theta}$ (the upper plot) and for the scale parameter $\log\sigma_{\theta}$ (the lower plot) respectively under the setting with time series length $t_{max} = 50$, average annual sample size $n = 25$, autocorrelation in θ_t $\phi_{\theta,\theta} = 0.4$ and 44 replications (50 replications were conducted, among which 6 replications report 3 or more divergent transitions for the MCMC of Bayesian inference and thus are removed from the analysis).

inference and Bayesian inference with Prior2, the latter two reported very close estimates for $\phi_{\theta,\theta}$. One striking thing is that the bias is close to or even larger than 0.4 for some replications, this suggests that the inferences report even negative estimates of $\phi_{\theta,\theta}$ and it again turns out to be a difficult parameter. In the lower plot, we can see no single inference technique stands out in estimating the scale parameter $\log\sigma_{\theta}$.

3.4 Prior-posterior distribution

Fig. 2 shows histograms of posterior samples of the scale parameter σ_{θ} from models with the two different prior distributions: half-Cauchy $(0, 10)$ and log-normal $(1, 0.5)$, which are represented by solid lines in the left and right plot on each subplot respectively. The true value of σ_{θ} is indicated by a solid red line. Plot (a), (b), (c) and (d) correspond to setting $(t_{max} = 25, n = 50)$, $(t_{max} = 25, n = 100)$, $(t_{max} = 50, n = 25)$ and $(t_{max} = 50, n = 100)$ respectively. We can see from plot (a) that the priors are quite informative and pull the posteriors towards small values away from the true value and this prior-domination is more clear with log-normal prior where the prior distribution sharply peaks at 2. The domination is not mitigated even though the mean annual sample size is increased to 100 as shown in plot (b). With the same total sample size in plot (c) $(t_{max} = 50, n = 25)$ as that in plot (a) $(t_{max} = 25, n = 50)$, the posterior likelihoods in plot (c) are, however, not dominated by the priors. The prior-domination is also mitigated in plot (d) compared with plot (b) by increasing the time points from

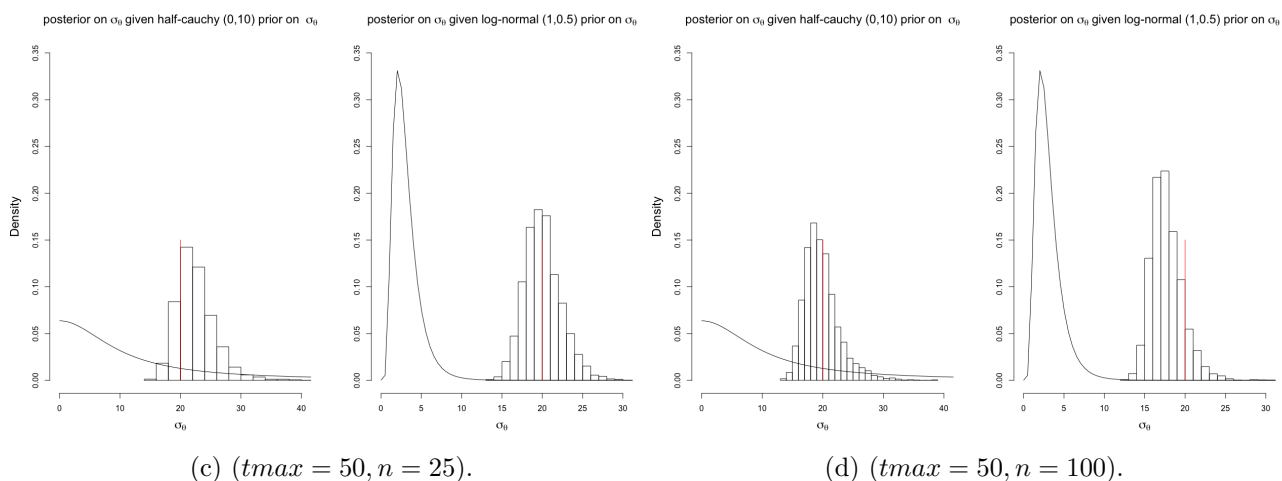
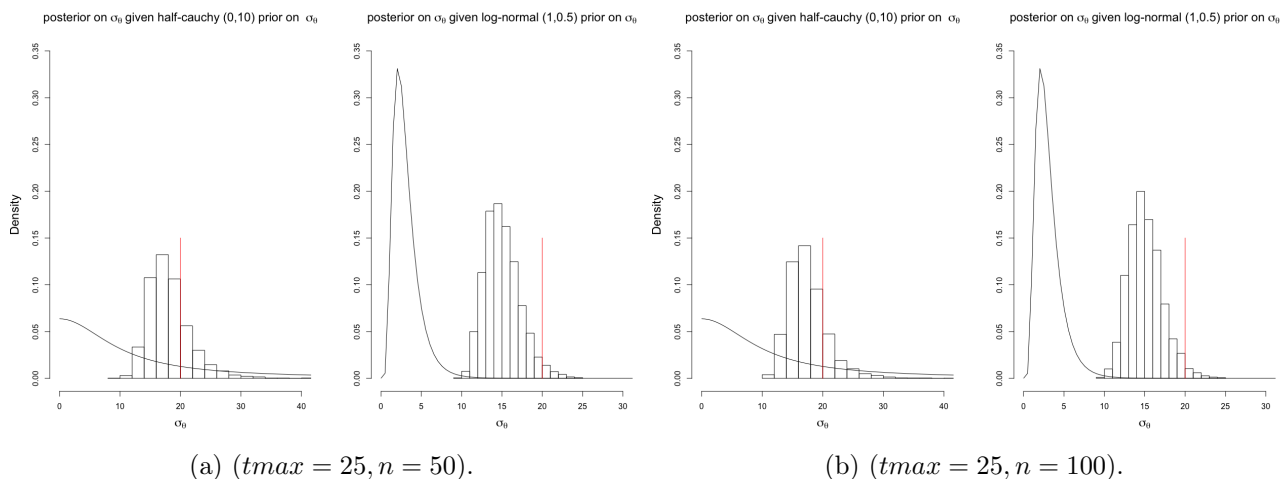


Figure 2: Histograms of posterior samples of the scale parameter σ_θ from models with two different prior distributions. Plot (a), (b), (c) and (d) correspond to sample size setting $(tmax = 25, n = 50)$, $(tmax = 25, n = 100)$, $(tmax = 50, n = 25)$ and $(tmax = 50, n = 100)$ respectively. On each subplot, the left one shows the histogram of posterior samples given half-Cauchy (0, 10) prior on σ_θ and similarly, the right one displays the histogram of posterior samples given log-normal (1, 0.5) prior on σ_θ . Overlaid on each subplot (the solid black lines) is the corresponding prior density function. The red lines indicate the true value of σ_θ . Only $\phi_{\theta, \theta} = 0.4$ was considered in the simulations.

25 to 50.

Altogether, the informative log-normal prior pulls more of the posterior towards a narrower range of smaller parameter values especially when the number of time points in the data is small. The posterior samples are less dominated by the half-Cauchy prior in this case. Increasing the annual mean sample size does not necessarily lead to better identification of the small region of parameter space. Only the amount of time points is the matter for the likelihood to overwhelm the prior distribution and to dominate the posterior distribution.

3.5 Computational efficiency with and without Laplace approximation

In *tmbstan*, sampling can be performed with or without Laplace approximation for the random effects. It is possible to mix the Laplace approximation with MCMC by specifying `laplace=TRUE`, such that the random effects are integrated with the Laplace approximation in TMB and other parameters (such as fixed effects and hyperparameters specifying the distribution of the random effects) are handled by the NUTS in Stan. In the case studies in Monnahan and Kristensen (2018), the Bayesian inference algorithms with Laplace approximation is less computationally efficient than without Laplace approximation, where the efficiency is defined as the minimum effective sample size per second. Following that definition, we calculated the efficiency of *tmbstan* with and without Laplace approximation with simulated data. Different from Monnahan and Kristensen (2018), we did not consider the computational efficiency of Frequentist inference with the Laplace approximation, as explained in the last section.

In Fig. 3, plot (a) displays violin plots of computational efficiency without (orange) and with (green) Laplace approximation (la) of Bayesian inference with Prior1 under different sample size settings. The setting 1, 2, 3, 4 on x axis stand for setting ($tmax = 25, n = 50$), ($tmax = 25, n = 100$), ($tmax = 50, n = 25$) and ($tmax = 50, n = 100$) respectively. Only $\phi_{\theta,\theta} = 0.4$ was considered and the divergent transitions were not taken into account. Inside the violin plots are box plots showing the quantiles of 50 realized computational efficiencies. Similarly, the violin plots of computational efficiency with Prior2 are shown on plot (b). We find from both plot (a) and (b) that Bayesian inference without Laplace approximation generally is more efficient under setting 1, 2, and 3, the outperformance is more manifest when the sample size is small ($tmax = 25, n = 50$). However, when the sample size is increased to ($tmax = 50, n = 100$), inference with Laplace approximation turns out to be slightly more efficient than that without Laplace approximation, the boxplots and violin plots also tend to be more compact under this setting.

Even though the technique in which the random effects are integrated out by Laplace approximation in TMB turns out to be less efficient in most settings, we still provide a counterexample from Monnahan and Kristensen (2018) in which the enabling of Laplace approximation is always less computationally efficient in the case studies.

3.6 Laplace approximation check

By comparing the Bayesian posteriors with and without Laplace approximation, we are allowed to check how well the Laplace approximation works. Fig. 4 shows pair plots of posterior samples with and without Laplace approximation done by TMB under different sample size settings with Prior2. Only autocorrelation in θ_t $\phi_{\theta,\theta} = 0.4$ was considered.

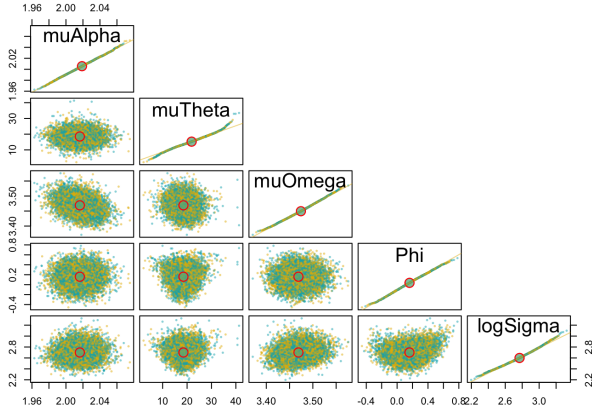


(a) Computational efficiency with Prior1.

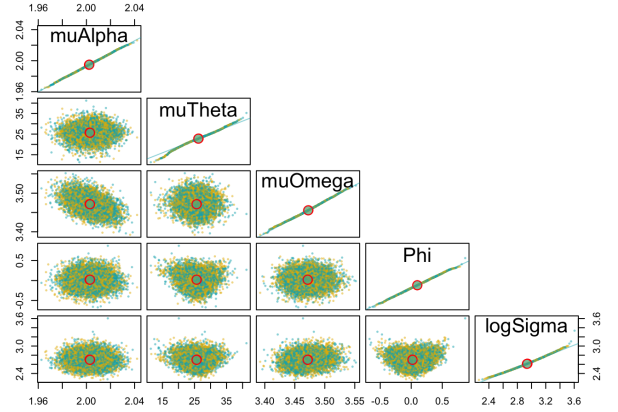


(b) Computational efficiency with Prior2.

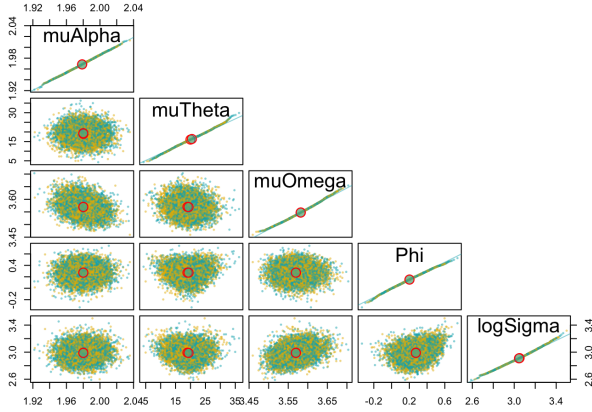
Figure 3: Violin plots of computational efficiency (minimum effective sample size per second) without (orange) and with (green) Laplace approximation (la). The four settings on x axis correspond to sample size setting ($tmax = 25, n = 50$), ($tmax = 25, n = 100$), ($tmax = 50, n = 25$) and ($tmax = 50, n = 100$) respectively. Plot (a) shows the computational efficiency of Bayesian inference with Prior1 and plot (b) with Prior2. Only $\phi_{\theta, \theta} = 0.4$ was used in simulations. Inside the violin plots are box plots showing the quantiles of 50 realized computational efficiencies. For each realization among the 50 simulations and across the settings, the same specifications in tmbstan are used.



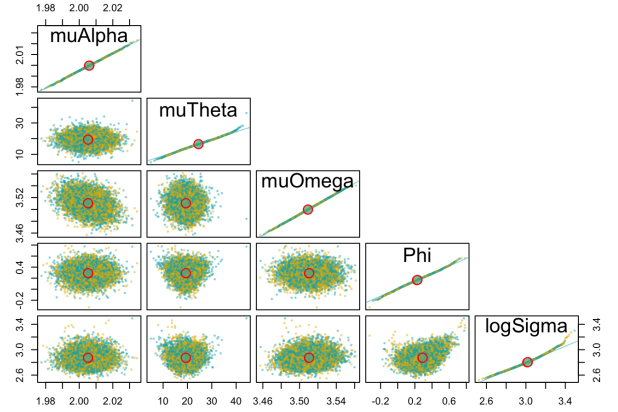
(a) ($t_{max} = 25, n = 50$) with Prior2.



(b) ($t_{max} = 25, n = 100$) with Prior2.



(c) ($t_{max} = 50, n = 25$) with Prior2.



(d) ($t_{max} = 50, n = 100$) with Prior2.

Figure 4: Pair plots of posterior samples for Laplace approximation check from one realization of the simulation with Prior2. The four plots (a) (b) (c) and (d) correspond to the four settings of sample size in simulation. The random effects in the TMB model can be integrated with two techniques: (1) full MCMC integration via NUTS and (2) Laplace approximation. To check the accuracy of Laplace approximation to the posterior likelihood density, the posterior samples for all the fixed effects in the model without (yellow dots) and with Laplace approximation (green dots) are shown pair-wisely on the same plot. Columns and rows on the lower diagonal correspond to pair-wise parameters, with the diagonal showing QQ-plot of posterior samples from Bayesian inference without (yellow dots) and with (green dots) Laplace approximation for that parameter including a 1:1 line in yellow. The large red circles on the off-diagonal plots represent the pairwise means. On each off-diagonal plot, there are 4000 yellow dots corresponding to 1000 samples retained from each of four chains without Laplace approximation, so as the green dots with Laplace approximation. Posterior rows were randomized to prevent consistent overplotting of one integration technique. Overlaps in the two colored dots suggest that the Laplace approximation is accurate.

Plot (a), (b), (c) and (d) correspond to setting $(tmax = 25, n = 50)$, $(tmax = 25, n = 100)$, $(tmax = 50, n = 25)$ and $(tmax = 50, n = 100)$ respectively. On each subplot, the lower diagonal plots contain pairwise parameter posterior points. The green dots represent posterior points from full MCMC integration via NUTS and the yellow points from enabled Laplace approximation of the random effects. The hollow red circles on the off-diagonal plots represent the pairwise means. The diagonal shows QQ-plot of posterior samples from Bayesian inference without (yellow dots) and with (green dots) Laplace approximation for that parameter including a 1:1 line in yellow. Even though the posterior points are densely packed, the overlap of the red circles with each technique shows seemingly good alignment of the two versions of the posterior, and this suggests that the Laplace approximation to the marginal likelihood where random effects are integrated out works well. Similar pair plots for Laplace approximation check with Prior1 can be found in Supporting Information.

4 Real-data case study

Having established the utility of our modeling approach and frequentist and Bayesian inference in the context of simulated data, we also applied the same statistical model to the analysis of a real great tit dataset of practical interest. The observed data were collected from a Dutch great tit (*Parus major*) population at the Hoge Veluwe National Park in the Netherlands (52°02' - 52°07'N, 5°51' - 5°32'E). The recorded variables include the number of chicks, number of fledglings, mother ID, brood laying date and so on for each brood. Laying dates are presented as the number of days after March 31 (day 1=April 1, day 31=May 1). Similar to Reed et al. (2013), only the broods with one or more chicks were considered in our analysis due to the high proportion (15.7%) of zero-observations in the number of fledglings among the broods. The number of fledglings was taken as the fitness component and assumed to be Poisson distributed. The analyzed dataset consists of brood records breeding in 61 years from 1955 to 2015 and the sample size in a specific year ranges from 10 to 164 with an average of 81 across the study years. See Reed et al. (2013) for more details on the study population and fieldwork procedures.

The focus of this empirical study is to compare the computational efficiency of Bayesian inference with and without Laplace approximation and to check the accuracy of Laplace approximation. However, since the true structure of the model is unknown, we first conducted model selection under the frequentist framework and the candidate models considered are different from each other only in the model structure of stochastic α_t , θ_t and ω_t . The details of all the candidate models including the best model are given in Supporting Information. We then made Bayesian inference with the two different priors as in the simulation study using the selected model. For each prior distribution, we implemented tmbstan with and without Laplace approximation to check the accuracy of Laplace approximation.

Table 2 lists the reported estimates of model parameters from maximum likelihood (MLE) and Bayesian estimates with half-Cauchy (0, 10) prior (Prior1) and log-normal (1, 0.5) prior (Prior2). The best model indicates VAR(1) structure of α_t and θ_t and non-zero correlation $\hat{\rho}_{\alpha,\theta}$. The width of stabilizing fitness function turned to be constant over the study years implied by zero $\hat{\omega}_t$. Frequentist inference and Bayesian inference with Prior2 report close estimates for $\phi_{\theta,\theta}$ but the estimates with Prior2 show again less uncertainty for most of the estimates except for $\rho_{\alpha,\theta}$. In terms of log σ_θ , Bayesian inference with Prior1

Table 2: Frequentist and Bayesian estimates of parameters in the selected model with great tit dataset. The Bayesian estimates (in column Prior1 and Prior2) are obtained without Laplace approximation done by TMB.

parameter	MLE	Prior1	Prior2
μ_α	2(0.0369)	2(0.0491)	2(0.0379)
μ_θ	18.5(5.35)	18.8(7.12)	19.4(5.09)
μ_ω	3.88(0.055)	3.89(0.0563)	3.86(0.0522)
$\phi_{\alpha,\alpha}$	0.379(0.12)	0.458(0.13)	0.398(0.124)
$\phi_{\theta,\theta}$	0.48(0.112)	0.545(0.114)	0.477(0.102)
$\log\sigma_\alpha$	-1.72(0.14)	-1.63(0.152)	-1.76(0.126)
$\log\sigma_\theta$	3.07(0.137)	3.16(0.155)	2.98(0.125)
$\rho_{\alpha,\theta}$	-0.728(0.0825)	-0.715(0.0895)	-0.661(0.0987)

Table 3: Comparison of computational efficiency between Bayesian inference without (in the row "Full MCMC") and with Laplace approximation (in the row "Laplace approximation") for random effects for the great tit case study.

Model	Inference	Time(s)	min.ESS	Efficiency(ESS/t)
Prior 1	Full MCMC	1542.215	186.7651	0.1211019
	Laplace approximation	15491.85	1004.643	0.06484975
Prior 2	Full MCMC	1266.096	291.0717	0.229897
	Laplace approximation	7815.218	1111.257	0.1421914

reports the largest estimate and least certainty compared with the other two techniques. The close resemblance between estimates of $\log\sigma_\theta$ based on maximum likelihood and Bayesian inferences suggests that the data contains a good amount of information on $\log\sigma_\theta$ so that the maximum likelihood overwhelms the log-normal prior and dominates the posterior likelihood.

Table 3 shows computational efficiencies of Bayesian inference without and with Laplace approximation. It turns out that the computational efficiency with Laplace approximation is approximately half of that without Laplace approximation in both models with Prior1 and Prior2.

Similar to Fig. 4, Fig. 5 and Fig. 6 display pair plots of posterior samples to check the accuracy of Laplace approximation with Prior1 and Prior2 respectively. Both the figures seemingly suggest a good mix of posterior samples with and without Laplace approximation for all the parameters in the selected model, indicating that the Laplace approximation assumption is met.

5 Conclusions and extensions

In this study, we have investigated frequentist inference and Bayesian inference with two different priors. The inferences were implemented with a state-space model estimating temporal fluctuating selection and with simulated biological data under four different simulation settings. A state-of-the-art R package (tmbstan) for fast fitting statistical models was used for Bayesian inference with Laplace approximation turning on or off. The simulation studies show that the choice of prior can have an important impact on the geometric

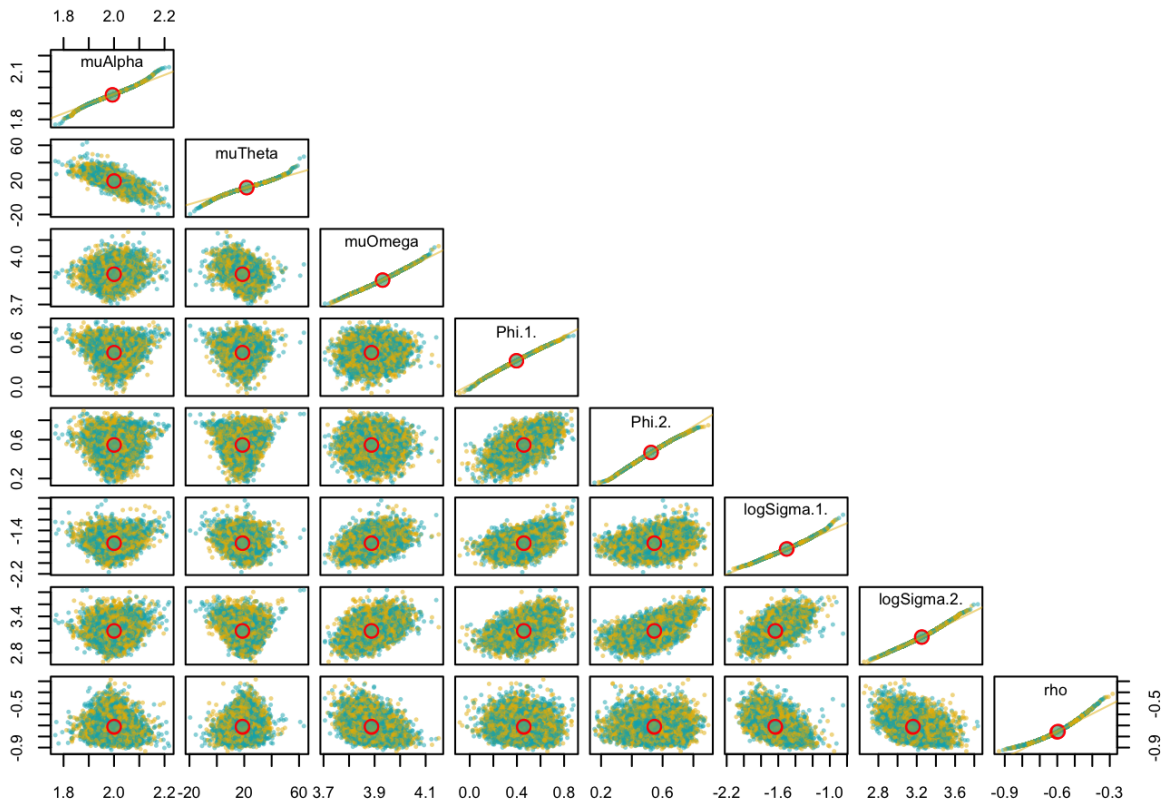


Figure 5: Pair plots of posterior samples for Laplace approximation test for the great tit case study with Prior1. The random effects in the great tit TMB model can be integrated with two techniques: (1) full MCMC integration via NUTS and (2) Laplace approximation. To check the accuracy of Laplace approximation to the posterior likelihood density, the posterior samples for all the fixed effects in the model without (yellow dots) and with Laplace approximation (green dots) are shown pair-wisely on the same plot. Columns and rows on the lower diagonal correspond to pair-wise parameters, with the diagonal showing QQ-plot of posterior samples from Bayesian inference without (yellow dots) and with (green dots) Laplace approximation for that parameter including a 1:1 line in yellow. The large red circles of the off-diagonal plots represent the pairwise means. On each off-diagonal plot, there are 4000 yellow dots corresponding to 1000 samples retained from each of four chains without Laplace approximation, so as the green dots with Laplace approximation. Posterior rows were randomized to prevent consistent overplotting of one integration technique. Overlaps in the two colored dots suggest the Laplace approximation assumption is met.

shape of the posterior distributions of the model parameters and a non-informative prior (in this study uniform prior and inverse-gamma prior on the scale parameter) may lead to unstable inference since the Markov chains may not converge or get stuck in part of the ridge of posterior. With unobserved states following a VAR(1) process, we also found that the autoregressive parameters and the scale parameters in the variance-covariance matrix of the states are difficult and challenging to be estimated accurately. The increased sample size at each time point does not necessarily provide more information for

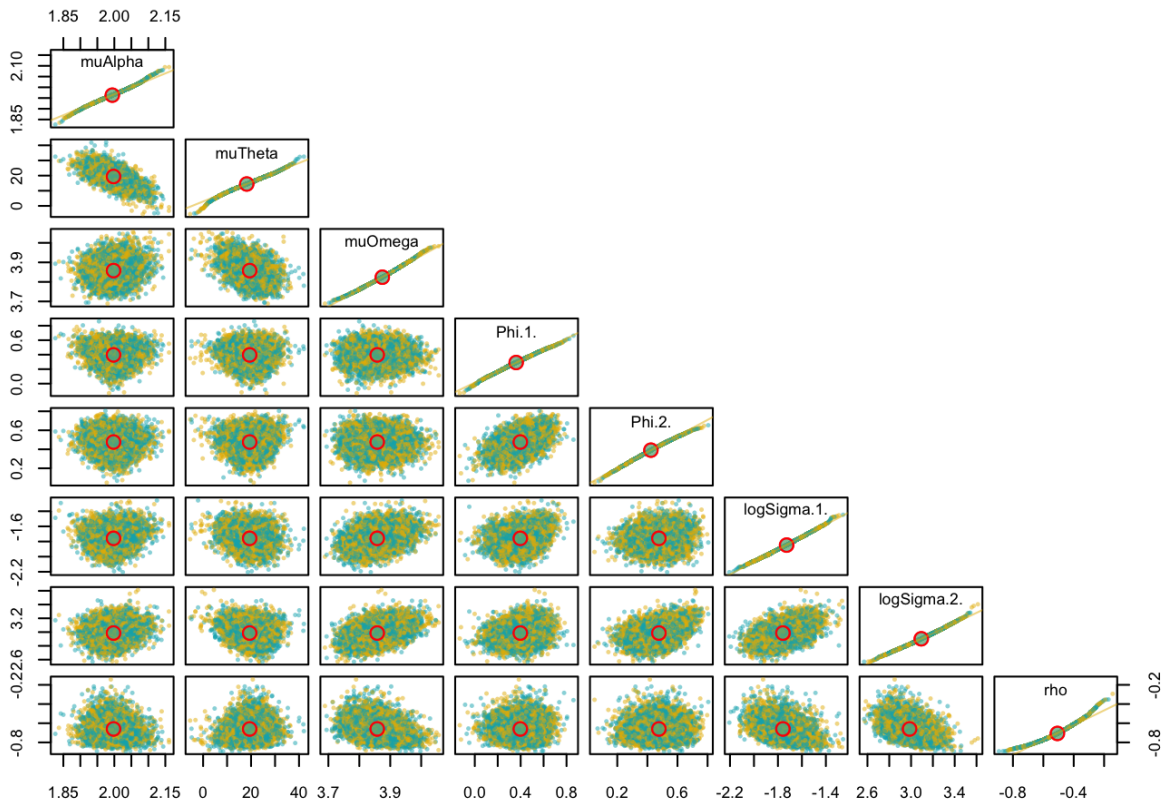


Figure 6: Pair plots of posterior samples for Laplace approximation test for the great tit case study with Prior2. The random effects in the great tit TMB model can be integrated with two techniques: (1) full MCMC integration via NUTS and (2) Laplace approximation. To check the accuracy of Laplace approximation to the posterior likelihood density, the posterior samples for all the fixed effects in the model without (yellow dots) and with Laplace approximation (green dots) are shown pair-wisely on the same plot. Columns and rows on the lower diagonal correspond to pair-wise parameters, with the diagonal showing QQ-plot of posterior samples from Bayesian inference without (yellow dots) and with (green dots) Laplace approximation for that parameter including a 1:1 line in yellow. The large red circles of the off-diagonal plots represent the pairwise means. On each off-diagonal plot, 4000 yellow dots correspond to 1000 samples retained from each of four chains without Laplace approximation, so as the green dots with Laplace approximation. Posterior rows were randomized to prevent consistent overplotting of one integration technique. Overlaps in the two colored dots suggest the Laplace approximation assumption is met.

the transition parameters and scale parameters. Only more time points in the data could make the likelihood dominate the posterior likelihood and thus lead to better estimates of these parameters. Half-Cauchy prior on the scale parameter leads to less stable inference than log-normal prior indicated by the number of divergent transitions in the Markov Chains. Laplace approximation for the random effects turns out to be accurate suggested by the pair plots of the posterior samples with and without Laplace approximation for both the simulation studies and the great tit case study. Turning on Laplace approxi-

mation in `tmbstan` would probably reduce computational efficiency but it is worth trying when there is a good amount of data, in which case the Laplace approximation is more likely to be accurate and also potentially improve the computational efficiency of MCMC.

In our study, we used arbitrary prior distributions, however, the prior information can be obtained from different sources. For example, in our great tit case study, the timing and width of the caterpillar peak can provide a clue for the time window of optimal laying dates, thus the information can be used to decide the prior for the scale parameter of the optimal laying dates. Prior information can also be generated from previous studies on the same species and more general ecological knowledge coming from other related species (Tufto et al., 2000).

We conducted simulation studies with only AR(1) process of the optimal laying dates, but the model is formulated and coded in a way that can be effortlessly extended to order-1 vector autoregression (VAR(1)). It can be widely used for modeling ecological processes where auto-correlation and cross-correlation in the processes arise due to shared environmental variables at either temporal or spatial scale. We expect more ecologists to adopt these two new estimation methods, TMB, and `tmbstan`, given its flexibility in either frequentist or Bayesian inference for a wide range of models, including the models where the unobserved ecological processes are treated as latent variables and assumed to be VAR processes. However, the drawback of Bayesian VAR (BVAR) methods is that it usually requires estimation of a large number of parameters and thus the over-parameterization might lead to unstable inference and inaccurate out-of-sample forecasts. Some shrinkage methods (Sims & Zha, 1998; Koop et al., 2010; Giannone et al., 2015; Sørbye & Rue, 2017, for example) were thereby developed, in which Bayesian priors provide a logical and consistent method of imposing parameter restrictions that can be potentially applied to ecological data cases.

References

- Albertsen, C. M., Nielsen, A., & Thygesen, U. H. (2016). Choosing the observational likelihood in state-space stock assessment models. *Canadian Journal of Fisheries and Aquatic Sciences*, *74*(5), 779–789.
- Auger-Méthé, M., Albertsen, C. M., Jonsen, I. D., Derocher, A. E., Lidgard, D. C., Studholme, K. R., . . . Flemming, J. M. (2017). Spatiotemporal modelling of marine movement data using Template Model Builder (TMB). *Marine Ecology Progress Series*, *565*, 237–249.
- Betancourt, M., & Girolami, M. (2015). Hamiltonian Monte Carlo for hierarchical models. *Current trends in Bayesian methodology with applications*, *79*, 30.
- Cadigan, N. G. (2015). A state-space stock assessment model for northern cod, including under-reported catches and variable natural mortality rates. *Canadian Journal of Fisheries and Aquatic Sciences*, *73*(2), 296–308.
- Cao, Y., Visser, M. E., & Tufto, J. (2019). A time-series model for estimating temporal variation in phenotypic selection on laying dates in a dutch great tit population. *Methods in Ecology and Evolution*, *10*(9), 1401–1411.
- Carpenter, B., Gelman, A., Hoffman, M. D., Lee, D., Goodrich, B., Betancourt, M., . . . Riddell, A. (2017). Stan: A probabilistic programming language. *Journal of statistical software*, *76*(1).
- Chevin, L.-M., Visser, M. E., & Tufto, J. (2015). Estimating the variation, autocorrelation, and environmental sensitivity of phenotypic selection. *Evolution*, *69*(9), 2319–2332.
- Fuglstad, G.-A., Hem, I. G., Knight, A., Rue, H., & Riebler, A. (2019). Intuitive principle-based priors for attributing variance in additive model structures. *arXiv preprint arXiv:1902.00242*.
- Gelman, A., Lee, D., & Guo, J. (2015). Stan: A probabilistic programming language for bayesian inference and optimization. *Journal of Educational and Behavioral Statistics*, *40*(5), 530–543.
- Gelman, A., et al. (2006). Prior distributions for variance parameters in hierarchical models (comment on article by Browne and Draper). *Bayesian analysis*, *1*(3), 515–534.
- Giannone, D., Lenza, M., & Primiceri, G. E. (2015). Prior selection for vector autoregressions. *Review of Economics and Statistics*, *97*(2), 436–451.
- Grant, P. R., & Grant, B. R. (2002). Unpredictable evolution in a 30-year study of Darwin’s finches. *science*, *296*(5568), 707–711.
- Hoffman, M. D., & Gelman, A. (2014). The No-U-Turn sampler: adaptively setting path lengths in Hamiltonian Monte Carlo. *Journal of Machine Learning Research*, *15*(1), 1593–1623.
- Jeffreys, H., & Jeffreys, H. (1961). *Theory of probability (3rd edn)*. Oxford.
- Karakani, H. M., van Niekerk, J., & van Staden, P. (2016). Bayesian analysis of AR (1) model. *arXiv preprint arXiv:1611.08747*.
- Koop, G., Korobilis, D., et al. (2010). Bayesian multivariate time series methods for empirical macroeconomics. *Foundations and Trends® in Econometrics*, *3*(4), 267–358.
- Kristensen, K., Nielsen, A., Berg, C. W., Skaug, H., & Bell, B. M. (2016). TMB: Automatic differentiation and Laplace approximation. *Journal of Statistical Software*, *70*(5), 1–21.

- Lei, G., Boys, R., Gillespie, C., Greenall, A., & Wilkinson, D. (2011). Bayesian inference for sparse VAR (1) models, with application to time course microarray data. *Journal of Biometrics and Biostatistics*.
- Lunn, D. J., Thomas, A., Best, N., & Spiegelhalter, D. (2000). WinBUGS—a Bayesian modelling framework: concepts, structure, and extensibility. *Statistics and computing*, 10(4), 325–337.
- Monnahan, C. C., & Kristensen, K. (2018). No-U-turn sampling for fast bayesian inference in ADMB and TMB: Introducing the admuts and tmbstan R packages. *PloS one*, 13(5), e0197954.
- Monnahan, C. C., Thorson, J. T., & Branch, T. A. (2017). Faster estimation of bayesian models in ecology using Hamiltonian Monte Carlo. *Methods in Ecology and Evolution*, 8(3), 339–348.
- Neal, R. M., et al. (2011). MCMC using Hamiltonian dynamics. *Handbook of markov chain monte carlo*, 2(11), 2.
- Reed, T. E., Jenouvrier, S., & Visser, M. E. (2013). Phenological mismatch strongly affects individual fitness but not population demography in a woodland passerine. *Journal of Animal Ecology*, 82(1), 131–144.
- Schlaifer, R., & Raiffa, H. (1961). *Applied statistical decision theory*. Wiley Cambridge.
- Sims, C. A., & Zha, T. (1998). Bayesian methods for dynamic multivariate models. *International Economic Review*, 949–968.
- Sørbye, S. H., & Rue, H. (2017). Penalised complexity priors for stationary autoregressive processes. *Journal of Time Series Analysis*, 38(6), 923–935.
- Stan Development Team. (2018a). Rstan: the R interface to stan. *R package version 2.17.3*. <http://mc-stan.org>.
- Stan Development Team. (2018b). Stan modeling language users guide and reference manual. *Version 2.18.0*. <http://mc-stan.org>.
- Tufto, J., Lande, R., Ringsby, T.-H., Engen, S., Sæther, B.-E., Walla, T. R., & DeVries, P. J. (2012). Estimating Brownian motion dispersal rate, longevity and population density from spatially explicit mark–recapture data on tropical butterflies. *Journal of Animal Ecology*, 81(4), 756–769.
- Tufto, J., Sæther, B.-E., Engen, S., Arcese, P., Jerstad, K., Røstad, O. W., & Smith, J. N. (2000). Bayesian meta-analysis of demographic parameters in three small, temperate passerines. *Oikos*, 88(2), 273–281.
- Vedder, O., Bouwhuis, S., & Sheldon, B. C. (2013). Quantitative assessment of the importance of phenotypic plasticity in adaptation to climate change in wild bird populations. *PLoS Biology*, 11(7), e1001605.
- Wei, W. (2006). *Time series analysis: Univariate and multivariate methods* (2nd ed.). Pearson Addison Wesley.
- Zellner, A. (1986). On assessing prior distributions and Bayesian regression analysis with g-prior distributions. *Bayesian inference and decision techniques*.